Physica Medica 57 (2019) 115–122

Contents lists available at ScienceDirect

Physica Medica

journal homepage: www.elsevier.com/locate/ejmp

Original paper

Development of geometrically ideal dose distribution as a reference for treatment planning in VMAT using filtered back-projection method

Kentaro Miki[a,*], Kazunari Hioki[b], Takeo Nakashima[b], Akito Saito[a], Yuji Murakami[a], Tomoki Kimura[a], Ikuno Nishibuchi[a], Yasushi Nagata[a]

[a] Department of Radiation Oncology, Hiroshima University Hospital, Japan
[b] Radiation Therapy Section, Department of Clinical Support, Hiroshima University Hospital, Japan

ARTICLE INFO

Keywords:
Optimization
Radiotherapy
Treatment planning
Volumetric-modulated arc therapy

ABSTRACT

Purpose: To determine optimal dose distribution in the treatment planning of volumetric modulated arc therapy (VMAT), a virtually ideal dose distribution was developed as a reference by applying filtered back-projection method.

Methods: Delineated structures in patient CT scans were identified using a treatment planning system. The projection of the planning target volume (PTV) was calculated along the X-ray direction for each angle of rotation. Each projection was Fourier transformed to the frequency space; a Shepp–Logan filter was applied, then an inverse Fourier transformation was performed. As the dose irradiation cannot assume a negative value, the filtered projections were shifted using the minimum value inside of the PTV. All values outside of the PTV were set to zero. The corrected filtered projections were then multiplied by the tissue-maximum ratio according to each voxel depth from the surface of the body to simulate X-ray attenuation. Finally, the distributions of multiple rotational angles were convolved to simulate the dose distribution of the VMAT.

Results: Ideal dose distributions were generated with sufficient uniformity inside of the PTV. Dose spreading except for the PTV due to external irradiation was reproduced in the case of a brain tumor. A reference dose distribution including OAR sparing was produced. The efficacy of this process as a target for optimum planning was confirmed.

Conclusion: Using applied filtered back-projection, the ideal dose distribution, which excluded some device-oriented restrictions, was generated. This application will provide support for the determination of VMAT planning quality by providing reference dose distributions.

1. Introduction

Recent developments in radiation therapy using X-rays has been predicated on mechanical or technical innovations of irradiation hardware or systems. Volumetric modulated arc therapy (VMAT) is one of the leading-edge techniques in radiation therapy. This approach is based on the modulation of multileaf collimator (MLC) during gantry rotation with continuous X-ray irradiation. VMAT results in efficient beam delivery and a higher dose conformity compared with conventional radiation therapy techniques [1,2]. Although high-precision treatment techniques are widely implemented in many facilities worldwide, it is expected that the volume of work required and the difficulty associated with treatment planning will increase. In VMAT planning, a commercial treatment planning system (TPS) is used to create an optimized environment with regard to dose distribution using an inverse planning process. This approach iteratively calculates the intensity of the distribution of photon beams to minimize a particular objective function. However, the typical parameters of the field configurations or objectives/constraints for each target structure have to be manually selected by planners by trial-and-error. In this process, planners need to determine the appropriate dose distribution with only their experience as guidance. To consistently determine the optimal dose distribution using an approach that is supported by objective methods, geometric ideal dose distributions could be useful as a reference.

In the dose calculation and optimization process, some restrictions need to be considered. They can generally be divided into three types; the first is related to the fundamental properties of particles, such as the

* Corresponding author at: Department of Radiation Oncology, Institute of Biomedical & Health Science, Hiroshima University, 1-2-3 Kasumi, Minami-ku, Hiroshima, Hiroshima 734-8551, Japan.
E-mail address: kentaro-miki@hiroshima-u.ac.jp (K. Miki).

https://doi.org/10.1016/j.ejmp.2018.12.034
Received 19 July 2018; Received in revised form 10 December 2018; Accepted 25 December 2018
Available online 04 January 2019

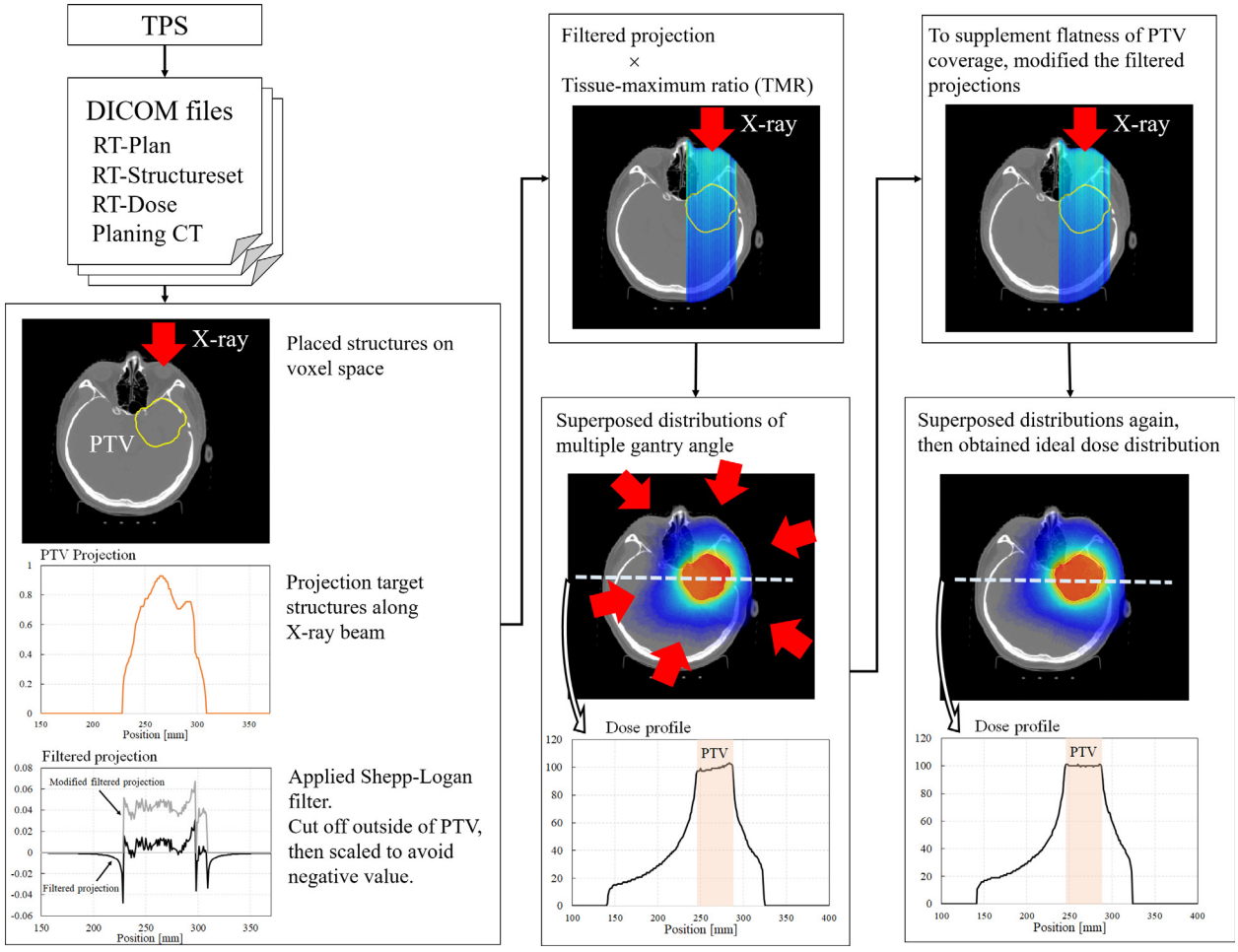

Fig. 1. Schematic drawing of workflow for depth dose calculation. *Abbreviations:* TPS = treatment planning system; RT = Radiotherapy; PTV = planning target volume.

Table 1
Dose constraints and priorities for treatment planning using isodose lines extracted from ideal dose distributions. Upper/Lower represent the dose limit. Relative priority was used and defined from 0 to 1000.

Target	Type	Dose [cGy]	Priority
PTV	Upper	5100	750
	Lower	5040	800
40 Gy	Upper	5000	250
	Lower	4000	200
30 Gy	Upper	4000	250
	Lower	3000	200
20 Gy	Upper	3000	300
	Lower	2000	200
10 Gy	Upper	2000	300
	Lower	1000	200

interaction between photons and other particles, the second involves medical factors such as the balance between target coverage and normal tissue sparing, and the third considers mechanical restrictions such as the modulation speed of the MLC or the dose rate. Although the restrictions that are attributable to the inherent properties of photons cannot be circumvented, it may be possible to effectively address the mechanical restrictions in the future by exploiting technical developments. Dose distribution, which is calculated by excluding mechanical restrictions, is related only to photon behavior in the body. Therefore, it should reflect the theoretical limits of geometrically feasible dose distribution. Moreover, in the planning optimization process, the geometrically ideal dose distribution would be useful as a reference. To calculate this distribution, we propose the application of the filtered back-projection method.

The method of image reconstruction using filtered back-projection is widely used in CT image reconstruction. The approach has some similarities to the dose distribution calculation; by considering the target structures as density distributions in the body, the filtered projections are compatible with the intensity distribution for each field. Unlike in image reconstruction, convolved dose distribution spreads the excess dose to the outside of the target structure because the intensity distribution cannot assume a negative value. To generate a uniform dose distribution inside of the target while reducing the dose to normal tissue, inverse treatment planning has been widely used in external beam radiotherapy. By applying a CT-like image reconstruction method without using negative values from the intensity distribution, the uniform dose distribution inside of the target together with the spreading of excess dose to the outside of the target could be simulated.

To optimize the convolved dose distribution, the applicability of filtered back-projection methods was previously examined, particularly in the case of Tomotherapy [3–6]. The recent development of optimization algorithms such as RapidArc (Varian Medical Systems, Palo Alto, CA) or Smart Arc (Philips Healthcare, Eindhoven, Netherlands) facilitates high-quality dose distribution within a practical time frame by exploiting recent developments in computing speed and sophisticated algorithms [7–10]. However, appropriate parameters for the optimized configurations are still selected manually, and the resultant dose distribution is subsequently reviewed by an oncologist, medical physicist

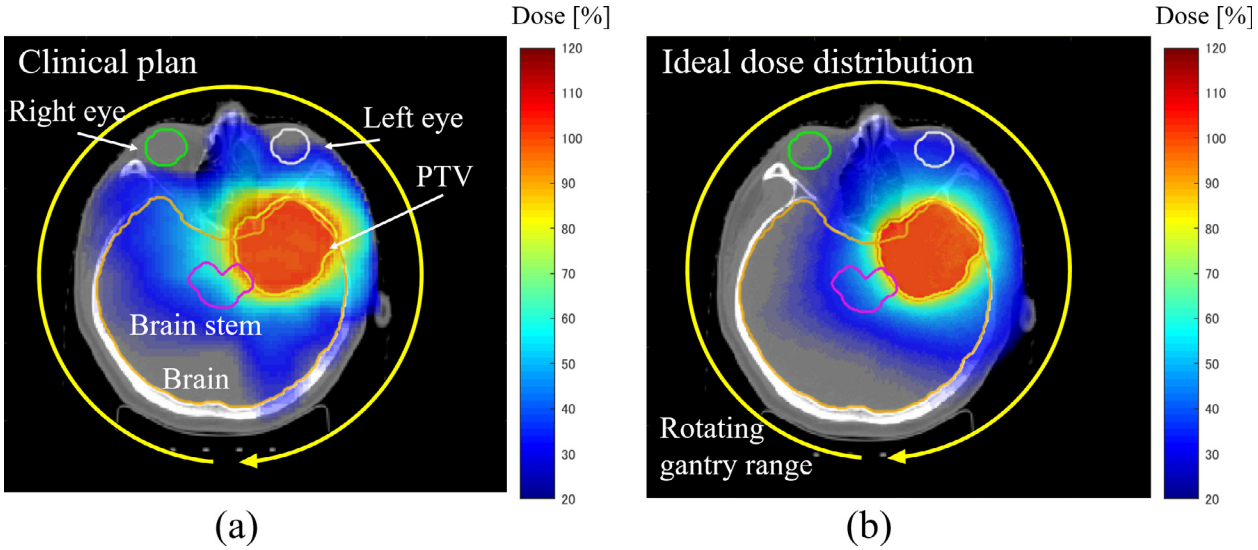

Fig. 2. Treatment planning for brain tumor patient (Patient 1) in the clinical case (a) and dose distribution calculated using the modified filtered back-projection method (b). Full rotating gantry angle (360°) was used.

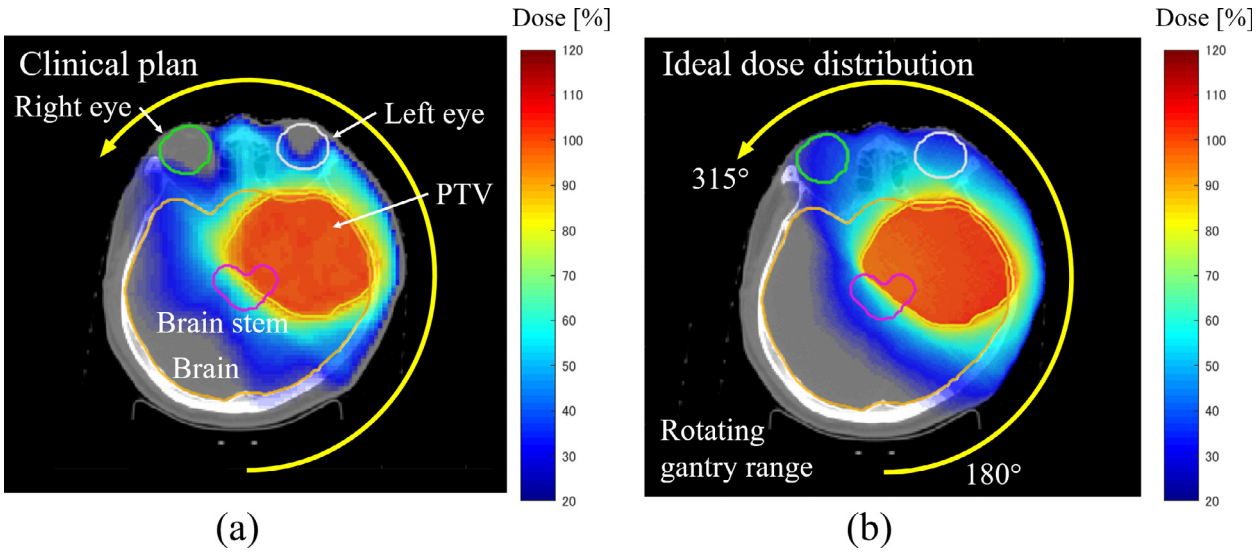

Fig. 3. Treatment planning for brain tumor patient (Patient 2) in the clinical case (a) and dose distribution calculated using the modified filtered back-projection method (b). Partial rotating gantry angle (180° to 315°) was used.

or dosimetrist, based on their experience. Therefore, the quality of treatment planning is heavily depended on the experience of the individual administering the treatment or the healthcare facility.

The aim of this study is to investigate the feasibility of applying the filtered back-projection method to produce geometrically ideal dose distributions as a reference for treatment planning of VMAT. To improve the efficiency and quality of VMAT planning via the development of supporting tools for the determination of optimal dose distribution, an ideal dose distribution calculator is proposed and evaluated.

2. Methods and materials

2.1. Calculation of ideal dose distribution

Generally, to determine the sinogram of a 2-D image generated from projections along the X-ray beam direction for each rotational angle, the Radon transform is employed. It is expressed as follows:

$$p(s,\theta) = \iint_{-\infty}^{\infty} f(x,y)\delta(x\cos\theta + y\sin\theta - s)dxdy$$

where, $f(x, y)$, $p(s, \theta)$, δ, and s represents the 2-D original image, the projection of $f(x, y)$, the delta function, and the distance of position $f(x, y)$ from the origin ($s = x\cos\theta + y\sin\theta$), respectively. According to the central slice theorem, a 2-D Fourier transform of an original image is equivalent to a 1-D Fourier transform of the projection $p(s, \theta)$, which can be expressed as follows:

$$\begin{aligned} F(x,y) &= \int\int_{-\infty}^{\infty} f(x,y)e^{-2\pi i(xX+yY)}dxdy \\ &= \int\int_{-\infty}^{\infty} f(x,y)e^{-2\pi i(x\rho\cos\theta+y\rho\sin\theta)}dxdy \\ &= \int_{-\infty}^{\infty} p(s,\theta)e^{-2\pi i\rho s}ds \\ &= P(\rho,\theta) \end{aligned}$$

where, $F(X, Y)$ represents the 2-D Fourier transform of $f(x, y)$, and $X = \rho\cos\theta$, $Y = \rho\sin\theta$. The original image is obtained from the inverse Fourier transform of $F(X, Y)$ as follows:

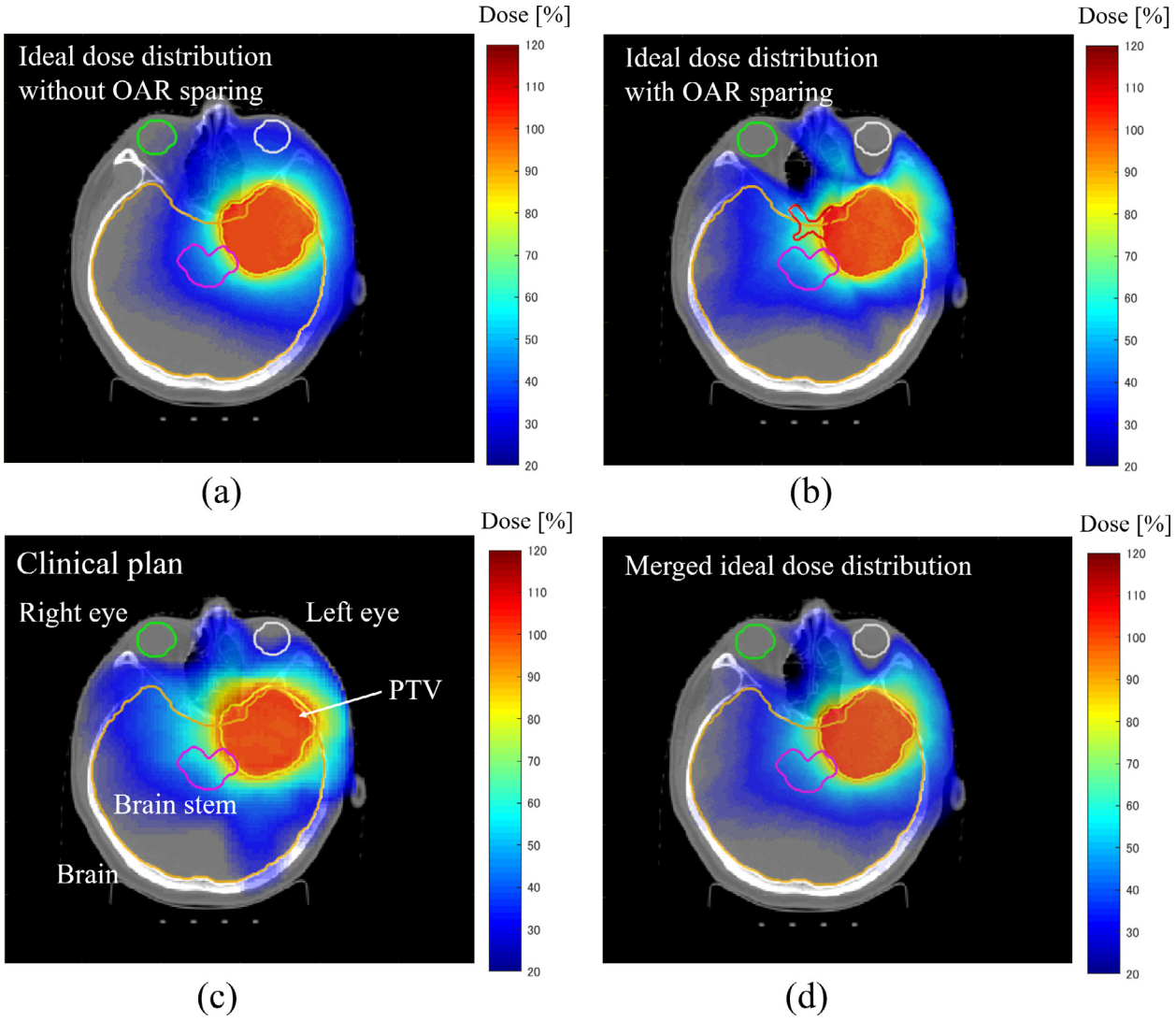

Fig. 4. Ideal dose distribution without OAR sparing (a), with OAR sparing (b), and clinical dose distribution of Patient 1 is shown in (c). The merged ideal dose distribution with $(1 - w) \times$ (a) $+ w \times$ (b) is shown in (d). $w = 0.35$ was used in this case.

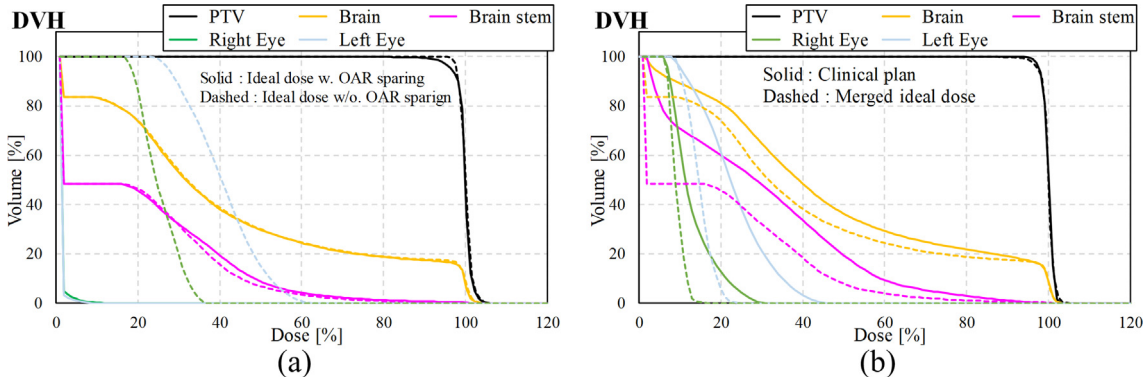

Fig. 5. DVHs of ideal dose distribution for Patient 1 with/without OAR sparing (a), and clinical plan/merged ideal dose distribution (b).

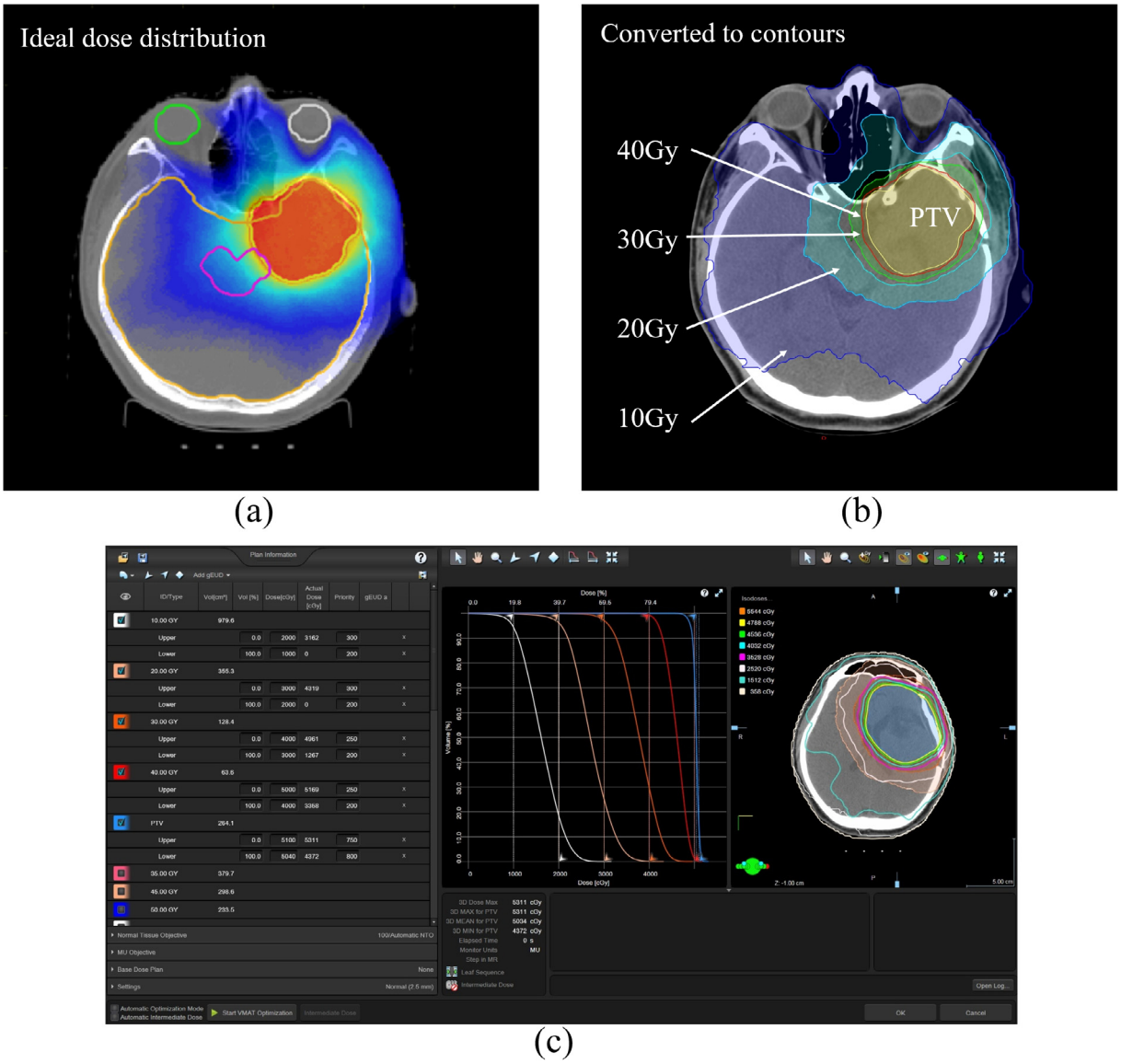

Fig. 6. To optimize the dose distribution using the ideal dose distribution (a), it is converted to contours (b). The screen shot of the commercial optimization tool (the Photon Optimization (PO-13716)) is shown in (c).

$$
\begin{aligned}
f(x,y) &= \int\int_{-\infty}^{\infty} F(X,Y)e^{2\pi i(xX+yY)}dXdY \\
&= \int_0^{2\pi}\int_0^{\infty} F(\rho\cos\theta,\rho\sin\theta)e^{2\pi i(x\rho\cos\theta+y\rho\sin\theta)}\begin{vmatrix}\frac{\partial X}{\partial\rho} & \frac{\partial X}{\partial\theta}\\ \frac{\partial Y}{\partial\rho} & \frac{\partial Y}{\partial\theta}\end{vmatrix}d\rho d\theta \\
&= \int_0^{2\pi}\int_0^{\infty} F(\rho\cos\theta,\rho\sin\theta)e^{2\pi i(x\rho\cos\theta+y\rho\sin\theta)}\rho d\rho d\theta \\
&= \int_0^{\pi}\int_{-\infty}^{\infty} P(\rho,\theta)|\rho|\, e^{2\pi i\rho s}d\rho d\theta
\end{aligned}
$$

Therefore, the original image can be reconstructed from a 1-D Fourier transform of the projection, $P(\rho,\theta)$, and the filter function $|\rho|$. In this study, the Shepp–Logan filter was adopted as the filter function instead of $|\rho|$. It is defined as:

$$
H(\rho) = \begin{cases} \frac{2\rho_n}{\pi}\left|\sin\left(\frac{\pi\rho}{2\rho_n}\right)\right| & ,|\rho| \le \rho_n \\ 0 & ,|\rho| > \rho_n \end{cases}
$$

where ρ_n represents the Nyquist frequency. When the 1-D Fourier transform of the projections of the contoured PTV are used as $P(\rho,\theta)$, the corresponding projections, $p(s,\theta)$, can be considered as the ideal X-ray bean intensity. The reconstructed image, $f(x,y)$ can then be interpreted as the dose distribution resulting from the projection beam intensities. Unlike the case of image reconstruction, the intensity of the external beam cannot assume negative values. Furthermore, X-rays will be attenuated inside the body. To avoid negative values, the inverse Fourier transform of the filtered projections was shifted using the minimum value of the result, and set to zero outside of the PTV.

$$
\text{off.} = \text{minimum}(P(\rho,\theta)|\rho|)
$$

$$
f(x,y)_{\text{shift}} = \begin{cases} \int_0^{\pi}\left(\int_{-\rho_n}^{\rho_n} P(\rho,\theta)H(\rho)e^{2\pi i\rho s}d\rho + |\text{off.}|\right)d\theta & ,p(s,\theta)\neq 0 \\ \int_0^{\pi}\int_{-\rho_n}^{\rho_n} 0\cdot e^{2\pi i\rho s}d\rho d\theta & ,p(s,\theta)=0 \end{cases}
$$

The inverse Fourier transform of the filtered projections was then multiplied by the tissue-maximum ratio (TMR), which is related to the distance of the surface of the body to each objective voxel in 2-D real space, to express the attenuation of the X-rays inside the body,

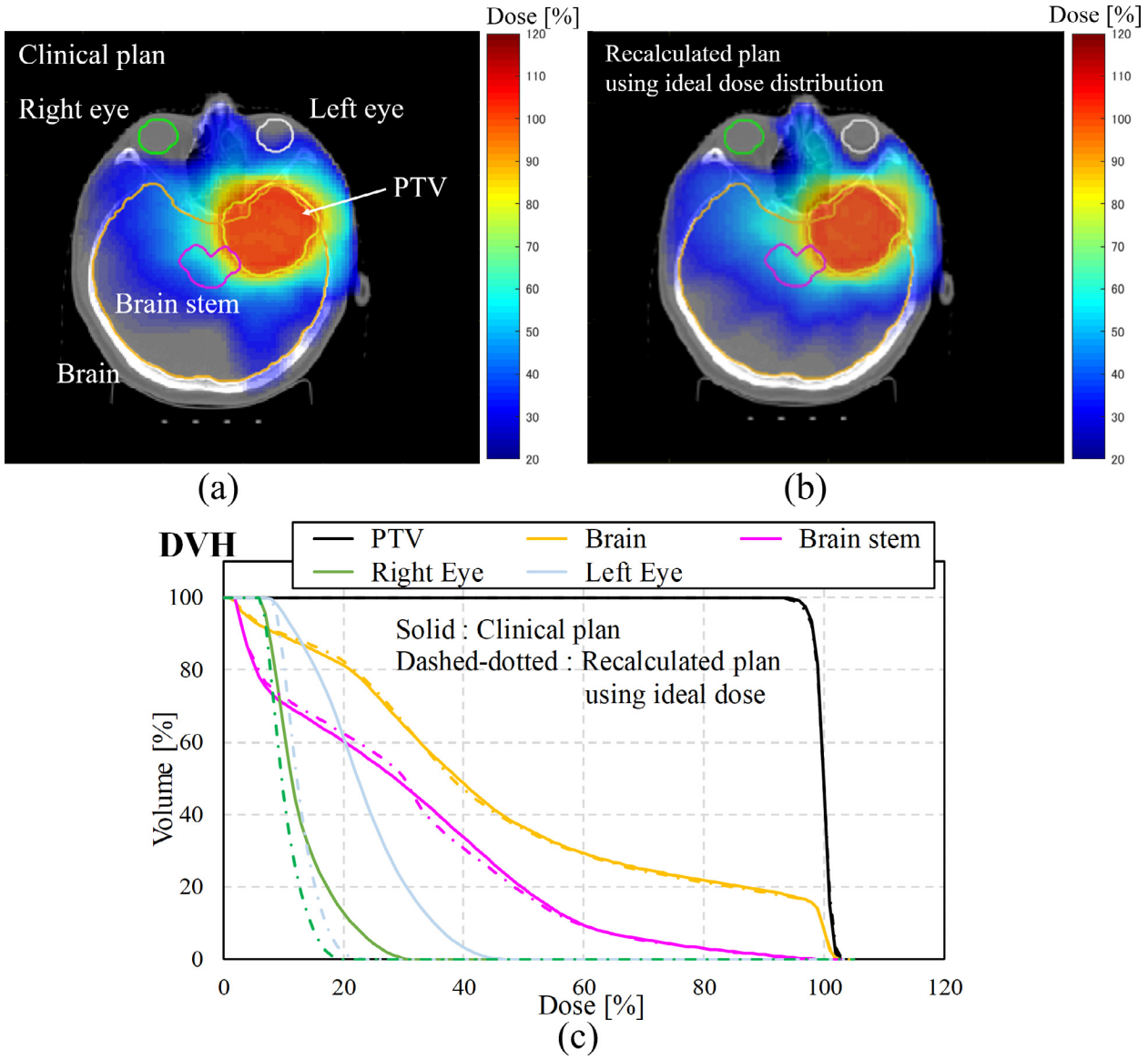

Fig. 7. Calculated dose distribution of Patient 1 using TPS (a), recalculated using ideal dose distribution as an optimization target using same TPS (b) and DVHs (c).

$$d(x, y) = \int_0^{\pi} \left(\int_{-\rho_n}^{\rho_n} P(\rho, \theta) H(\rho) e^{2\pi i \rho s} d\rho + |\text{off.}| \right) \text{TMR}(s, \theta) d\theta,$$

the application of the TMR renders the 2-D distribution of the inverse Fourier transform non-symmetric with respect to θ;

$$g(\theta) = \left(\int_{-\rho_n}^{\rho_n} P(\rho, \theta) H(\rho) e^{2\pi i \rho s} d\rho + |\text{off.}| \right) \text{TMR}(s, \theta) \neq g(\theta + \pi)$$

therefore, $d(x, y)$ calculated by integration over θ from 0 to π, is not homogeneous within PTV. To compensate for the lack of flatness over the PTV, the integration range over θ was increased to 2π. Since this integration was performed discretely via numerical calculations, the equation for $d(x, y)$ would be rewritten as following;

$$d(x, y) = \sum_{\theta=0}^{2\pi} \left(\int_{-\rho_n}^{\rho_n} P(\rho, \theta) H(\rho) e^{2\pi i \rho s} d\rho + |\text{off.}| \right) \text{TMR}(s, \theta).$$

The Inverse Fourier transform of $P(\rho, \theta)$ was superposed in 1° steps in this study. The calculation of both the Fourier transform and inverse Fourier transform was performed using the built-in fast Fourier transform function in MATLAB (version 9.2, The MathWorks Inc., Natick, MA). Finally, the obtained distribution, $d(x, y)$, was normalized by the average voxel value inside of the PTV to the prescribed dose.

$$D(x, y) = d(x, y) \cdot \frac{\text{Prescribed dose}}{\text{Average of voxel values}}$$

The reconstructed image, $D(x, y)$, represents the geometrically ideal dose distribution. Due to the employed X-ray attenuation term of the TMR, the flatness of the PTV coverage is insufficient, especially in the case where the PTV is located on the edge of the body. To compensate for the lack of flatness, we extracted the difference between $D(x, y)$ and the 2-D original image that satisfied the PTV prescription criteria, $f(x, y)$, and then added $f(x, y)$ to this difference. The pixels outside of the PTV were set to zero based on the following conditions:

$$f_{(2)}(x, y) \equiv \begin{cases} f(x, y) + \{f(x, y) - D(x, y)\} & , x \in PTV \cap y \in PTV \\ 0 & , x \notin PTV \cup y \notin PTV \end{cases}$$

The suffix value of function f indicates the number of iterations. The difference of $f(x, y) = f_{(1)}(x, y)$ and $f_{(2)}(x, y)$ is considered to be an artificial PTV prescription that the algorithm must start from to establish the desired clinical prescription. The PTV 2-D image $f(x, y)$ was replaced with $f_{(2)}(x, y)$ and the same process was repeated from the Radon transform. The resultant reconstructed image $D_{(2)}(x, y)$ calculated using $f_{(2)}(x, y)$ instead of $f(x, y)$ should be more uniform. In most cases, a single iteration ($D_{(2)}(x, y)$) was sufficient to establish a uniform

dose distribution with enough accuracy. This 2-D dose distribution was repeatedly calculated in the superior–inferior direction of the patient using the same processes; then the 3-D ideal dose distribution was generated. To avoid a large computational cost, the influence of photon scattering was excluded from this estimation. For comparison with a clinical plan, the dose volume histogram (DVH) was calculated. A schematic drawing of the calculation workflow is shown in Fig. 1.

2.2. Data acquisition and analysis

We performed this investigation using the CT data of patients with brain tumors who were scheduled to receive radiation treatment by VMAT at our hospital. Prior to commencement, this study was reviewed and approved by the Institutional Review Board at our hospital. CT images were acquired using a 16 multislice CT scanner (Light Speed® 16-slice; GE Healthcare, Waukesha WI, USA) and imported to TPS (Eclipse, Varian Medical Systems, Palo Alto, CA). Radiation oncologists contoured the gross tumor volume (GTV) and added margins to define the clinical target volume (CTV) and the planning target volume (PTV) for each patient. These target volumes were manually modified as necessary. The delineated structures for the brain, brain stem, and eyes were identified as the organs at risk (OARs), in this study. Delineated structures in patient CT scans were exported from the TPS in DICOM format. The patient body and planning target volume (PTV) were placed in a 3-D voxel space using the original CT image. The voxel size was 512, and the pixel spacing was 0.977 mm for each axis, while the pixel spacing in the clinical plan was 2.5 mm. The calculation code was written using MATLAB.

Initially, the ideal dose distribution for a 360° rotating gantry angle was calculated using VMAT planning data. The data set for astrocytoma, a 35-year-old male, was analyzed (Patient 1). The CTV was an enlarged isotropic 1 cm from the GTV, and the PTV was an enlarged isotropic 5 mm from CTV. The size of the PTV was 264.1 cm^3. The prescribed dose was planned at 50.4 Gy par 28 fractions for the PTV. The calculated dose was normalized to the dose at 50% of the PTV (PTV-D50%).

Thereafter, the partial gantry angle case was determined. The dataset for astrocytoma, a 39-year old, male was processed (Patient 2). The CTV was an enlarged isotropic located 1 cm from the GTV, and the PTV was an enlarged isotropic 3 mm from the CTV. The size of the PTV was 320.2 cm^3. The prescribed dose was planned at 50.4 Gy par 28 fractions for PTV. Two arcs from 180° to 315° rotating gantry angles were used in the clinical planning (the angle count was initiated from vertically upward in the clockwise direction of the gantry). The calculated dose was normalized to PTV-D50%.

To implement our ideal dose distribution as a useful tool in clinical practice, the design of the shape of the dose distribution including the constraints on the OAR must be established. On the other hand, it is difficult to suggest a single absolute solution because the balance of the target coverage and OAR sparing is depended on the clinical decision. In this study, we calculated both the distribution of the non-sparing OAR and complete sparing by masking the 1-D Fourier transform projection, $P(\rho, \theta)$, on the location of the OAR projection. Then, the merged dose distribution is calculated by blending these distributions with a specific ratio as follows:

$$d(x, y)_{\text{OAR sparing}} = \begin{cases} \sum_{\theta=0}^{2\pi} \left(\int_{-\rho_n}^{\rho_n} P(\rho, \theta) H(\rho) e^{2\pi i \rho s} d\rho + |\text{off.}| \right) \text{TMR}(s, \theta) \\ \qquad , p(s, \theta) \neq 0 \cap o(s, \theta) = 0 \\ \sum_{\theta=0}^{2\pi} \int_{-\rho_n}^{\rho_n} 0 \cdot e^{2\pi i \rho s} d\rho d\theta \\ \qquad , p(s, \theta) = 0 \cup o(s, \theta) \neq 0 \end{cases}$$

$$D(x, y)_{\text{merge}} = w \bullet D(x, y) + (1 - w) \bullet D(x, y)_{\text{OAR sparing}}$$

where w and $o(s, \theta)$ represent the ratio of blending ($0 \leq w \leq 1$) which is defined case by case, and the 1-D projection of a typical OAR, respectively. By adjusting w, the sparing level could be appropriately chosen. In this study, we will demonstrate the ideal dose distribution including OAR sparing using the data set of Patient 1 with a clinically used plan.

2.3. Distribution based optimization

By generating the ideal dose distribution including OAR sparing, it could be used as a target for dose distribution optimization. The ideal dose distribution is converted to contours using Velocity (Varian Medical Systems, Palo Alto, CA), and imported to TPS. Isodose lines were extracted for 10, 20, 30, and 40 Gy. The dose constraints and priorities used are summarized in Table 1. Optimization was performed using the Photon Optimization algorithm (PO-13716, Varian Medical Systems, Palo Alto, CA). To confirm the efficacy of this process, the resultant dose distribution was compared with a clinical plan.

3. Results

The dose distribution calculated using the modified filtered back-projection method was determined based on a comparison with the clinically used plan in Fig. 2. A full rotating gantry angle (360°) was utilized and the uniform dose distribution inside the PTV was confirmed. Dose spreading, except for the PTV due to the external X-ray irradiation, was reproduced by simulating the photon attenuation and using the geometric relationship of PTV inside the body. This approach also could be applied to a partial arc plan (Fig. 3). An anisotropic shape of the dose distribution was generated. By applying the compensated calculation for the flatness (previously described as $D_{(2)}(x, y)$), high uniformity could be established even for a partial arc plan.

In clinical practice, a good balance between target coverage and sparing OARs has to be considered. To employ the OAR sparing function in the workflow, we calculated both the ideal dose distributions with and without OAR sparing. The dose distributions are shown in Fig. 4(a) and (b), and the DVHs are shown in Fig. 5(a). The balance of target coverage and OAR sparing depends on the clinical determinations. In this study, the clinical plan was consulted to establish the balance with OAR sparing. Fig. 4(d) shows the blended ideal dose distribution with ratio w for the ideal dose without OAR sparing and $(1 - w)$ for the ideal dose with OAR sparing. To reduce or maintain the value of the eye dose as the clinical plan, $w = 0.35$ was used. The DVHs of the clinical plan and the merged ideal dose are shown in Fig. 5(b). If mechanical restrictions can be ignored, the dashed line of the DVH would be obtained by dose optimization calculation (in other words, this is one of the goals of dose optimization). We can easily determine if well-optimized planning is achieved or not by using this approach in optimization practice.

To perform optimization using the ideal dose distribution, the ideal dose distribution was converted to contours (Fig. 6(a) and (b)). The contours were imported to TPS and optimization was performed (Fig. 6(c)) for these contours as the optimization targets. It was also possible to add the constraints for other structures to the optimization items if necessary. The resultant dose distribution using the contours of the ideal dose distribution is shown in Fig. 7(b) for comparison with a clinical plan (Fig. 7(a) and (c)). The dose distribution with an additional reduction of eyes doses was obtained while PTV coverage was not compromised.

4. Discussion

In this study, an original tool to produce geometrically ideal dose distributions as a reference for the determination of the optimum dose distribution in VMAT planning was developed. A high level of uniformity was generated inside the PTV by applying a CT-like filtered back-projection process. Dose spreading except for the PTV due to

external X-ray irradiation was reproduced by simulating photon attenuation inside the body using TMR. This approach could be applied to partial arc planning using the same process. We also demonstrated how to spare OARs using this approach, although the constraints of critical organs need to be a clinical determination for each case. As one of the effective use of ideal dose distribution, distribution-based optimization was performed and the high quality of the resultant dose distribution was confirmed. It should also be possible to apply this approach to non-coplanar planning by adding a couch rotating term.

In the treatment planning workflow, some parameters of optimization configurations need to be manually selected, or the template and the resultant dose distribution have to be reviewed based on clinical experience. To establish an efficient clinical workflow or fully automated treatment planning system, some reference data would be helpful in determining the resultant dose distribution. In recent studies on this subject, a knowledge-based treatment system was introduced and clinically acceptable results were reported [11,12]. However, the quality of treatment planning using such methods will depend on the quality of the library that is used. Therefore, a large number of high-quality treatment plans is required prior to implementation. Our approach would also contribute to the development of an automated planning system as the determination tool for the calculated dose distribution, in combination with another approach. We believe that such an adjunctive tool would contribute to efficient, well-conceived plans with a more objective motivation because it is only depended on the geometric relationship of the patient's body, PTV, and OARs.

This would be useful not only for providing the reference dose distribution, given that the usage for distribution-based optimization is another key feature. In the general optimization process, planners indicated the values of the dose constraint (such as maximum dose, minimum dose, or mean dose) and gave priority to TPS for each target. To indicate a more detailed shape of the dose distribution, it is necessary to identify some supporting targets. By converting the ideal dose distribution to contours with the same format as the other structures of the organs, we can use this information as the dose optimization target in commercial TPS. Modification of the ideal dose structures and the addition of the organ structures as optimization constraints are also possible. We demonstrated this process using a patient case and confirmed a greater reduction of OAR doses without degrading PTV coverage. By producing the ideal distribution as the optimization target, it is possible to indicate the preferable distribution to TPS more directly.

The processing time of the current version was approximately 1.5 h for 1 cycle, (360° rotating gantry range with 1° steps) with a pixel size of 512 × 512 × 512 using a mid-range performance laptop computer (Intel Core dual i7 CPU, 16 GB RAM). By optimizing the code or rewriting native code, reducing the pixel size or employing parallel computing, the computational burden can be sufficiently reduced to facilitate daily clinical use.

The influence of heterogeneity correction or X-ray scattering was not considered to reduce the computational burden in this study. The errors related to the filtered back-projection or the discrete rotational gantry angle could also be considered as a source of systematic uncertainty. Although the details of the dose distribution should be different for our estimated and the actual doses, we believe that the ideal dose distribution as the supporting tool for the determination of calculated dose using TPS is useful for improved efficiency and quality of treatment planning for VMAT.

5. Conclusion

We developed an ideal dose distribution to determine the treatment planning of VMAT by applying the filtered back-projection method. This facilitates a high level of dose uniformity inside of the PTV in addition to dose spreading, except for the PTV due to external irradiation. Such a supporting tool would contribute to the efficient production of optimum distribution on a more objective basis.

Conflict of interest

None.

Acknowledgement

We would like to thank Editage (www.editage.jp) for English language editing.

Funding sources

This research did not receive any specific grant from funding agencies in the public, commercial, or not-for-profit sectors.

References

[1] Otto K. Volumetric modulated arc therapy: IMRT in a single gantry arc. Med Phys 2008;35:310–7.
[2] Verbakel W, Cuijpers JP, Hoffmans D, Bieker M, Slotman BJ, Senan S. Volumetric intensity-modulated arc therapy vs. conventional IMRT in head-and-neck cancer: a comparative planning and dosimetric study. Int J Radiat Oncol Biol Phys 2009;74:252–9.
[3] Bortfeld T, Burkelbach J, Boesecke R, Schlegel W. Methods of image-reconstruction from projections applied to conformation radiotherapy. Phys Med Biol 1990;35:1423–34.
[4] Holmes T, Mackie TR. A filtered backprojection dose calculation method for inverse treatment planning. Med Phys 1994;21:303–13.
[5] Holmes TW, Mackie TR, Reckwerdt P. An iterative filtered backprojection inverse treatment planning algorithm for tomotherapy. Int J Radiat Oncol Biol Phys 1995:1215–25.
[6] Shepard DM, Ferris MC, Olivera GH, Mackie TR. Optimizing the delivery of radiation therapy to cancer patients. SIAM Rev 1999;41:721–44.
[7] Cozzi L, Dinshaw KA, Shrivastava SK, Mahantshetty U, Engineer R, Deshpande DD, et al. A treatment planning study comparing volumetric arc modulation with RapidArc and fixed field IMRT for cervix uteri radiotherapy. Radiother Oncol 2008;89:180–91.
[8] Vanetti E, Nicolini G, Nord J, Peltola J, Clivio A, Fogliata A, et al. On the role of the optimization algorithm of RapidArc (R) volumetric modulated arc therapy on plan quality and efficiency. Med Phys 2011;38:5844–56.
[9] Lee TF, Chao PJ, Ting HM, Lo SH, Wang YW, Tuan CC, et al. Comparative analysis of SmartArc-based dual arc volumetric-modulated arc radiotherapy (VMAT) versus intensity-modulated radiotherapy (IMRT) for nasopharyngeal carcinoma. J Appl Clin Med Phys 2011;12:158–74.
[10] Feygelman V, Zhang G, Stevens C. Initial dosimetric evaluation of SmartArc - a novel VMAT treatment planning module implemented in a multi-vendor delivery chain. J Appl Clin Med Phys 2010;11:99–116.
[11] Chanyavanich V, Das SK, Lee WR, Lo JY. Knowledge-based IMRT treatment planning for prostate cancer. Med Phys 2011;38:2515–22.
[12] Good D, Lo J, Lee WR, Wu QJ, Yin FF, Das SK. A Knowledge-based approach to improving and homogenizing intensity modulated radiation therapy planning quality among treatment centers: an example application to prostate cancer planning. Int J Radiat Oncol Biol Phys 2013;87:176–81.